Microscopic interpretation of inelastic electron scattering from even Ni isotopes

Atsushi Yokoyama
Laboratory of Physics, School of Medicine, Teikyo University, Hachioji, Tokyo 192, Japan

Kengo Ogawa
Laboratory of Physics, Kanto Gakuin University, Yokohama, Kanagawa 236, Japan

(Received 17 May 1990)

Transition charge densities of inelastic electron scattering for the excitation of 2^+ and 4^+ states in even-mass Ni isotopes are investigated in terms of the standard shell model of the $(p_{3/2},p_{1/2},f_{5/2})^n$ configurations. Effective transition operators pertinent to the model space are derived by considering particle-hole excitations up to $12\hbar\omega$ for $C2$ and $14\hbar\omega$ for $C4$ transitions within the framework of a first-order perturbation theory. It is shown that surface-peaked transition charge densities can be obtained for the first excited 2^+ and 4^+ states, being in agreement with experiment. Particle-hole excitations up to $\lambda\hbar\omega$, e.g., $\lambda=2$ for $C2$ transition, are most responsible for that feature. Higher $\hbar\omega$ excitations appear relatively significant in the interior region of the nucleus: They enhance the peak around the surface, improving further agreement with experiment, but for $C2$ transition they tend to generate another peak inside the nucleus and thus seem to deteriorate agreement with experiment. Transition densities for the $0^+_{g.s.}\rightarrow 2^+_{2,3}$ and $0^+_{g.s.}\rightarrow 4^+_2$ transitions are also discussed.

I. INTRODUCTION

Electron scattering is unequaled for the investigation of nuclear structure.[1] The cross sections for the scattered electrons, measured up to sufficiently high momentum transfer region, can be transformed into the charge and current densities between the initial and final states by taking the Fourier-Bessel transform of the form factors.[2] Thus, ample information on the radial structure of a nucleus can be obtained in comparison with usual gamma transitions.

Considerable amounts of experimental data of inelastic scattering have been accumulated in recent years and transition charge densities $\rho^{tr}(r)$ have been extracted for low-lying states in various nuclei.[2-4] It has been shown that the $\rho^{tr}(r)$ for collective states such as 2^+ and 3^- states are characterized by their prominent peak at the nuclear surface. A macroscopic model, e.g., the Tassie model derived from the liquid drop model, is often used to analyze experimental data on transition charge densities, because the $\rho^{tr}(r)$ is defined by a first derivative of the ground-state charge density that is usually assumed to be the Fermi distribution and therefore the $\rho^{tr}(r)$ is necessarily a surface peak.[1] From a microscopic viewpoint, on the other hand, there is no *a priori* reason why $\rho^{tr}(r)$ should have a surface-peaked shape. A sophisticated theory is needed in order to interpret the characteristic feature of $\rho^{tr}(r)$. In addition, $\rho^{tr}(r)$ for noncollective states, which do not necessarily seem to be a surface-peaked shape, may provide a stringent test of such a microscopic model.

In the nuclear shell model, one must first truncate a complete Hilbert space in order to make a calculation viable and then introduce a model space that consists of a sufficiently small number of valence orbitals (v). An orbit that is higher in energy than a valence orbit may be called an empty orbit (e), and an orbit being lower than a valence orbit may be referred to as a filled orbit (f), which is usually assumed to be completely filled by nucleons to make an inert core. Once wave functions, consisting of the valence orbitals only, are obtained, e.g., by diagonalizing Hamiltonian matrices, any observables such as electromagnetic transition probabilities can be calculated by use of those wave functions. Electromagnetic properties must therefore be described by using effective operators instead of free-nucleon operators in order to compensate the truncation of the Hilbert space. An effective charge is a typical example, which is widely used in phenomenological approaches and has been shown to be very successful in correlating many $E\lambda$ properties. Horie and Arima[5,6] considered its microscopic origin as coming from excitations of particles of the type f$\rightarrow$v, f$\rightarrow$e, and v$\rightarrow$e, by using a first-order perturbation theory. They calculated the quadrupole moments of odd-mass nuclei[5] and obtained fairly good agreement with experiments except for the nuclei with very large quadrupole moments. The f$\rightarrow$e excitation, i.e., the particle-hole (p-h) excitations from the filled orbits (core) to the empty orbits, is now known to give a dominant contribution to the effective charges, which is often referred to as core polarization. Application of the theory to inelastic electron scattering (longitudinal component) was made by several authors.[7,8]

For singly-closed-shell nuclei, in which only one kind of nucleon is considered to be active, the nuclear shell model is very successful to correlate a number of nuclear properties with relatively small numbers of phenomenological parameters. Ni isotopes provide us with one of the good examples of such nuclei and several calculations have so far been carried out within the $(p_{3/2},p_{1/2},f_{5/2})^n$ configurations,[9] where $n=A-56$, with A being the mass number, is the number of neutrons distributed in

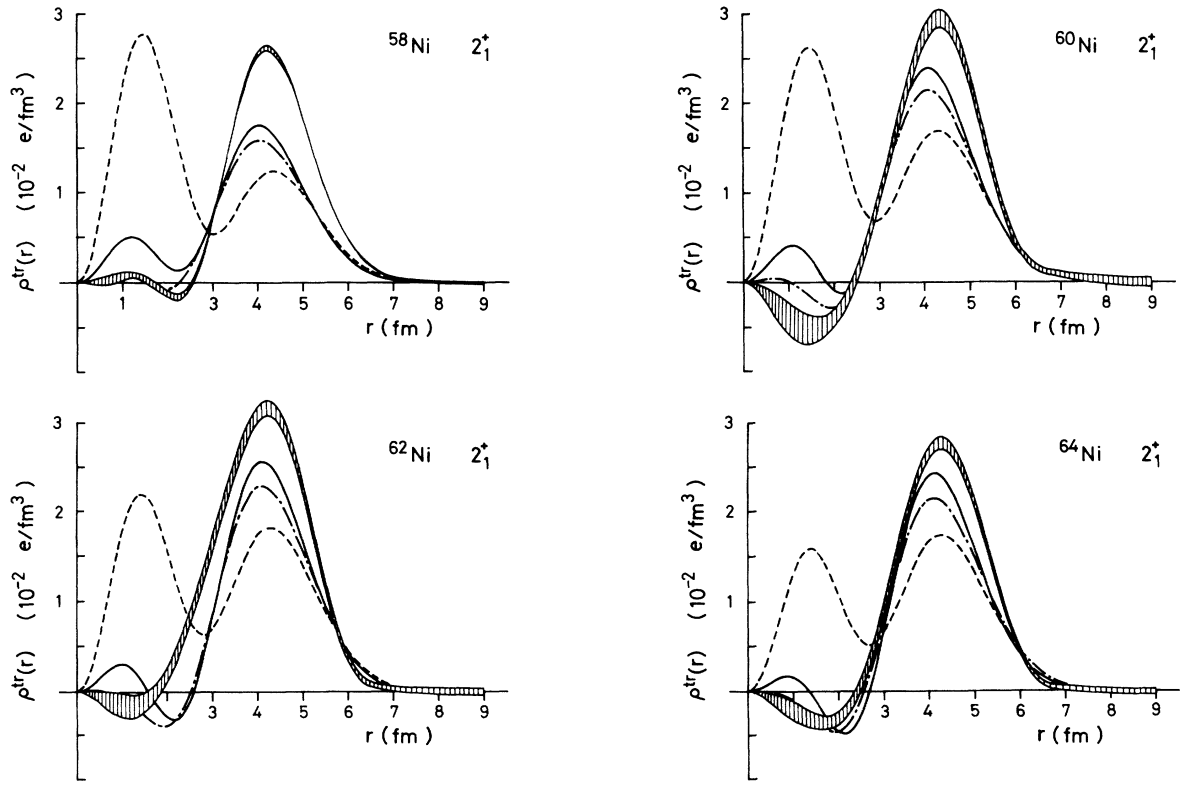

FIG. 1. Calculated and experimental (Ref. 2) transition charge densities $\rho^{tr}(r)$ for the first excited 2^+ states of even-mass Ni isotopes. The M3Y is used as the mixing interaction. The broken curve denotes the calculations with the constant neutron effective charge of 1.0e. The dot-dashed and solid curves are obtained from the configuration-mixing calculations up to $2\hbar\omega$ and $12\hbar\omega$ p-h excitations, respectively. The experimental transition charge densities are shown by the shaded area.

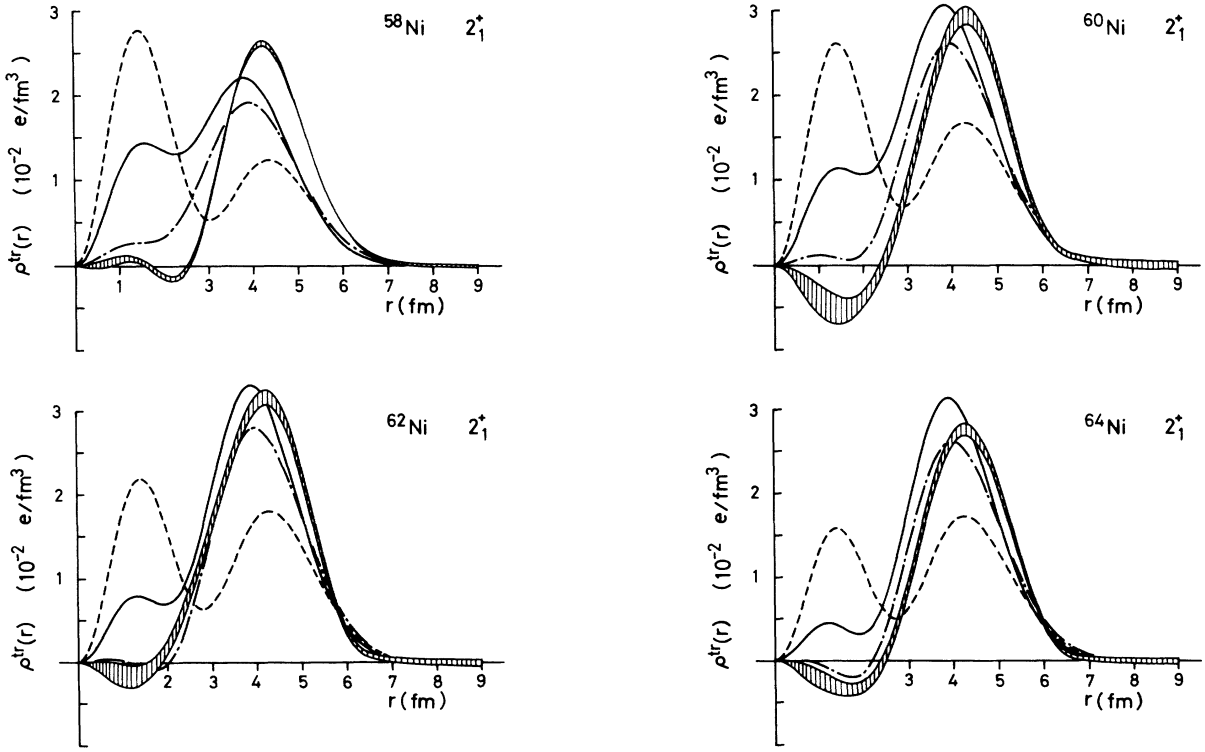

FIG. 2. Calculated and experimental (Ref. 2) transition charge densities $\rho^{tr}(r)$ for the first excited 2^+ states of even-mass Ni isotopes. The ST is used as the mixing interaction. See caption to Fig. 1.

the valence orbit outside an inert ^{56}Ni core. If one assumes the effective charge of $1.7e$ for all active neutrons, experimental data on $E2$ transitions and Q moments are nicely explained. It is a natural extension to apply the same theory to interpret the $\rho^{\rm tr}(r)$ for the first excited 2^+ states of even Ni isotopes. It turns out that there appear two peaks in the $\rho^{\rm tr}(r)$ and the one inside the nucleus is larger in lighter Ni isotopes than the other at the surface [$R \simeq (60)^{1/3} \sim 4$ fm], as shown in Figs. 1 and 2. This is a strong contradiction to the observed $\rho^{\rm tr}(r)$ characterized by a prominent surface peak, as mentioned before, suggesting that the phenomenological effective charge does not work well. It seems therefore that deriving effective $C\lambda$ operators from a microscopic theory is particularly interesting and would provide useful information to deepen the idea of effective charges.

The purpose of this paper is to consider the particle-hole (p-h) excitations of the ^{56}Ni core in order to understand the transition charge densities of Ni isotopes within the framework of the standard shell model. A first-order perturbation theory is adopted in order to take account of the p-h excitations to generate effective transition operators. Since the model space of the neutron configurations allows only proton excitations of f$\rightarrow$e type for $E\lambda$ properties, those contributions can be renormalized into a one-particle operator in a certain condition, and the concept of effective charge itself, as usually adopted in phenomenological approaches, is still valid.[10] Our discussion would thus be almost identical to that on momentum-transfer dependence of effective charges as well as state dependence. It is another purpose of this paper to apply our theoretical approach to the other transitions such as $0^+_{\rm g.s.} \rightarrow 2^+_{2,3}$ and $0^+_{\rm g.s.} \rightarrow 4^+_{1,2}$ transitions and discuss them in connection with the nuclear-structure models.

Federman and Zamick[11] and Rimini[12] performed configuration-mixing calculations on effective charges for $E2$ transitions in Ni isotopes, and they found that there exists considerable state dependence at a photon point. A broken-pair model calculation was made[13] for ^{58}Ni within the $(0+2)\hbar\omega$ model space and a surface-peaked $\rho^{\rm tr}(r)$ is obtained for the $0^+_{\rm g.s.} \rightarrow 2^+_1$ transition due to the $2\hbar\omega$ excitations. A Brief Report on the calculations for the transition densities for the 2^+_1 states of Ni isotopes has recently been published elsewhere.[14]

II. RESULTS AND DISCUSSIONS

The electron scattering formulas used in the present calculations are found in Refs. 1 and 2, while the method of perturbation calculations is given in Ref. 14. Formulas expressing the experimental transition charge densities and their errors assumed in the present calculations are given in the Appendix. We present the results mainly with the mixing interactions of M3Y (seven ranges with r^2 Yukawa)[15] and ST (Schiffer-True with four ranges).[16]

A. Convergence

The radial function in the operator for the $C\lambda$ transition is $j_\lambda(qr)$ and thus the matrix element $(nl|j_\lambda(qr)|n'l')$ calculated with use of the harmonic oscillator wave functions does not vanish, even when the difference of the principal quantum number between the initial and final states $\Delta N = |2n + l - (2n' + l')|$ exceeds $\lambda\hbar\omega$, contrary to the matrix element of r^λ in the usual $E\lambda$ gamma transitions. We have made configuration-mixing calculations up to $\lambda\hbar\omega$ and $(\lambda+10)\hbar\omega$ p-h excitations in order to see how perturbative terms converge. The convergence can in general depend on momentum transfer q. Contributions from each $k\hbar\omega$ p-h excitation at $q = 0.7$ fm^{-1} for the $0^+_{\rm g.s.} \rightarrow 2^+_1$ $C2$ transition and those at $q = 1.1$ fm^{-1} for the $0^+_{\rm g.s.} \rightarrow 4^+_1$ $C4$ transition in ^{60}Ni are shown in Fig. 3, as a typical example for the transitions to the 2^+_1 and 4^+_1 states in Ni isotopes. Around those q values, the form factors take their first peak. It can be readily seen that the $2\hbar\omega$ p-h excitations give the largest contribution in the perturbation calculations, and the contributions from the $2\hbar\omega$ and $0\hbar\omega$ excitations dominate in this q region. At $q \approx 1.6$ fm^{-1}, the second peak of the form factors for the $C2$ transition, the higher $\hbar\omega$ components become more significant than those in the lower q region, but the $2\hbar\omega$ and the $0\hbar\omega$ contributions are still large and their combined contribution dominates in the perturbed matrix elements. The perturbed matrix elements up to $q \sim 2$ fm^{-1} converge very rapidly as one takes higher $\hbar\omega$ excitations into account, and the gross feature of $\rho^{\rm tr}(r)$ around the surface is determined by those matrix elements. Therefore, we assume that taking up to the $(\lambda+10)\hbar\omega$ excitation would be large enough to get a sufficient convergence in order to make a qualitative discussion on $\rho^{\rm tr}(r)$, particularly around the surface. It should be pointed out that the matrix elements in the $q \geq 2$ fm^{-1} region come mostly from the higher $\hbar\omega$ excitations and have significant influence on the $\rho^{\rm tr}(r)$ inside the nucleus, and therefore the convergence in the interior region would become worse than that around the surface region.

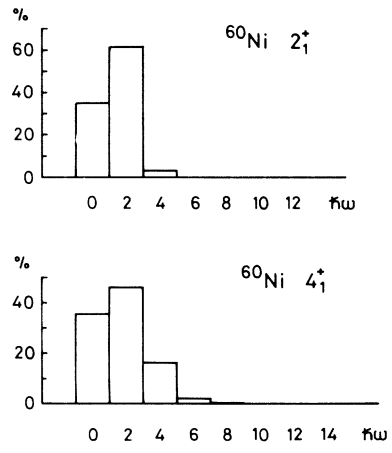

FIG. 3. Contributions from each $k\hbar\omega$ p-h excitation in the perturbed matrix elements for the $0^+_{\rm g.s.} \rightarrow 2^+_1$ $C2$ transition at $q = 0.7$ fm^{-1} and for the $0^+_{\rm g.s} \rightarrow 4^+_1$ $C4$ transition at $q = 1.1$ fm^{-1} in ^{60}Ni, given in percent. The momentum transfer assumed gives roughly the first peak of each form factor. The M3Y is used as the mixing interaction.

B. $0^+ \rightarrow 2_1^+$

Figures 1 and 2 summarize the calculated and experimental[2] transition charge densities for the first excited 2^+ states of ^{58,60,62,64}Ni, where the M3Y and ST are used, respectively, as the mixing interactions for the perturbation calculations. The calculations are made with the three different assumptions on the effective transition operators, (1) a constant effective charge, (2) perturbation up to $2\hbar\omega$, and (3) perturbation up to $12\hbar\omega$. The same shell-model wave functions are used in these calculations, which are obtained from the $(p_{3/2},p_{1/2},f_{5/2})^n$ configurations[9] with the best fitted effective interaction matrix elements and give a good account of energy spectra. The crudest model assumes the constant effective charge for neutrons, and neither state nor q dependence is considered there. We adopt $e_n = 1.0e$ in Figs. 1 and 2 for the sake of comparison with the other calculations, though $e_n = 1.7e$ is needed to fit the matrix elements at the photon point or around the first peak of the form factors. This prescription predicts the transition charge density with a large peak inside the nucleus, as mentioned at the beginning, for all the 2_1^+ states of the Ni isotopes. The large inside peak in the $\rho^{\rm tr}(r)$, for example, for ^{58}Ni, corresponds to the broad peak ranging from $q = 1.5$ to 3.0 fm^{-1} in the form factor, and the radial matrix element $(p|j_2(qr)|p)$ is responsible for this picture. The $p \rightarrow p$ contribution is dominant in the $0_{\rm g.s.}^+ \rightarrow 2_1^+$ transition matrix elements, as far as the $(p_{3/2},p_{1/2},f_{5/2})^n$ configurations are assumed. In the heavier Ni isotopes, however, the matrix element $(f_{5/2}|j_2(qr)|p)$ becomes appreciable and the peak inside the nucleus is getting smaller. It is thus clear from this phenomenological point of view that either q dependence of e_n or extension of the model space, e.g., including the $f_{7/2}$ as an active orbit,[17,18] must be considered explicitly.

The $\rho^{\rm tr}(r)$ calculated with the perturbation up to $2\hbar\omega$ and $12\hbar\omega$ p-h excitations are shown in Fig. 1 with the M3Y and in Fig. 2 with the ST. The significant feature of these calculations is that there appears the surface peak in the $\rho^{\rm tr}(r)$ and the $\rho^{\rm tr}(r)$ in the interior region of the nucleus is considerably depressed. It thus seems that both the $2\hbar\omega$ and $12\hbar\omega$ calculations agree with experiments much better than the calculations with the constant effective charge. The position of the surface peak tends to be shifted slightly toward the interior region of the nucleus in the calculations with the ST, as shown in Fig. 2, but this can be remedied by the slight change in the oscillator constant in calculating the transition matrix elements.

Figure 4 presents each contribution to $\rho^{\rm tr}(r)$ from the $0\hbar\omega$, $2\hbar\omega$, and $(0+2)\hbar\omega$ p-h excitations separately, where the $0\hbar\omega$ contribution includes the p-h excitations from the $f_{7/2}$ to the remaining fp orbitals. The $\rho^{\rm tr}(r)$ of ^{60}Ni only is illustrated here, since the $\rho^{\rm tr}(r)$ of the other Ni isotopes is similar to that. The $0\hbar\omega$ contribution has a node: Its contribution inside the nucleus and that around the surface differ in their phase. The $2\hbar\omega$ contribution to the $\rho^{\rm tr}(r)$ is essentially a Gaussian shape centered around the surface, but it has a small but non-negligible bump around $r \sim 1.5$ fm. Around the nuclear surface $R \sim 4$ fm,

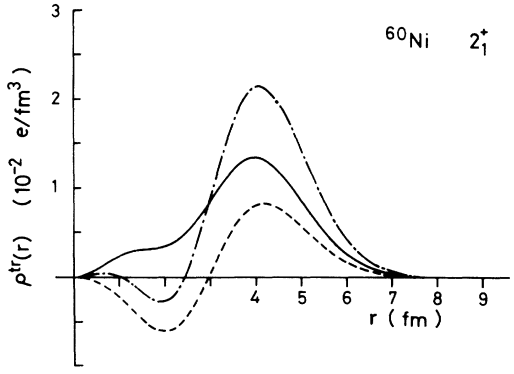

FIG. 4. Contributions from the $0\hbar\omega$, $2\hbar\omega$, and $(0+2)\hbar\omega$ p-h excitations are shown separately for $\rho^{\rm tr}(r)$ for the $0_{\rm g.s.}^+ \rightarrow 2_1^+$ transition in ^{60}Ni. The M3Y is used as the mixing interaction. The broken curve and the solid curve denote the contributions from the $0\hbar\omega$ and $2\hbar\omega$ excitations, respectively. The dot-dashed curve indicates the $(0+2)\hbar\omega$, i.e., the sum of the $0\hbar\omega$ and $2\hbar\omega$ contributions.

the $0\hbar\omega$ and $2\hbar\omega$ contributions are added in phase, whereas inside the nucleus the two contributions cancel each other. Therefore, as shown by the $(0+2)\hbar\omega$ calculations, a large peak can be obtained around the surface and the $\rho^{\rm tr}(r)$ in the interior region is significantly depressed, which generates a sharp surface-peaked shape expected for the $\rho^{\rm tr}(r)$ for collective states. This feature is almost independent on the mixing interactions employed.

High Fourier components of the matrix elements can be brought in by the mixing of the higher $\hbar\omega$ ($> 2\hbar\omega$) p-h excitations. By comparing the $2\hbar\omega$ calculations with the $12\hbar\omega$ ones, it is easily seen from Figs. 1 and 2 that the higher $\hbar\omega$ components give rise to an appreciable change in the $\rho^{\rm tr}(r)$ inside the nucleus and to an increase of the $\rho^{\rm tr}(r)$ around the surface. In the interior region of the nucleus, since the $0\hbar\omega$ and $2\hbar\omega$ contributions cancel each other, the contributions from the higher $\hbar\omega$ excitations become relatively apparent. There appears another bump or peak, which is not in agreement with experiment. This feature is more apparent in the calculations with the ST than with the M3Y. In the calculations with the ST, the bump in the $\rho^{\rm tr}(r)$ at $r \sim 1.5$ fm coming from the $2\hbar\omega$ contribution becomes larger and deviates apparently from a Gaussian shape, being another ingredient to deteriorate the agreement with experiment inside the nucleus. If one employs the other mixing interactions such as the delta force, the Gaussian central, and the Yukawa central, the calculated results also give an appreciable peak inside the nucleus, particularly significant for lighter Ni isotopes. It seems therefore that the dependence on the mixing interactions appears more crucial in the interior region of the nucleus and in the lighter-mass Ni isotopes.

Contributions from the central, LS, and tensor forces are examined, by using the M3Y and ST interactions. It is shown that the central force plays a dominant role, and noncentral forces are not important, as far as the $0_{\rm g.s.}^+ \rightarrow 2_1^+$ transitions are concerned.[14]

Shell-model calculations of Ni isotopes with extended model space were carried out by the Utrecht group,[17,18]

in which the one-particle excitations from the $f_{7/2}$ to the remaining fp orbitals were taken into account in the model space. The $\rho^{tr}(r)$ is calculated[4] for the various excited states in ^{58}Ni. The constant additional effective charges of $1.0e$ are assumed both for protons and neutrons. The defect of the $(p_{3/2},p_{1/2},f_{5/2})^n$ calculations in which only the neutron degrees of freedom are considered is remedied appreciably due to the $f_{7/2}\rightarrow p_{3/2}$ contribution, but there still remains a significant peak in the $\rho^{tr}(r)$ inside the nucleus. This means clearly that the $0\hbar\omega$ contribution only is not sufficient and more than $2\hbar\omega$ p-h excitations should be considered explicitly. As demonstrated by the present configuration-mixing calculations, it is the $2\hbar\omega$ p-h excitations that are responsible for giving the surface-peaked shape for the $\rho^{tr}(r)$ for the 2_1^+ states of even-mass Ni isotopes.

In the present calculations, however, the $0\hbar\omega$ p-h excitations, which play an important role, have relatively large mixing amplitudes. The mixing amplitude squared for some of the $(\alpha\|\tilde{O}^{(\lambda)}\|\beta)$ amounts to roughly 10%. It should be better to treat the $f_{7/2}$ orbit, i.e., the $0\hbar\omega$ p-h excitations in a nonperturbative way. A calculation within the $r^n+r^{n+1}f_{7/2}^{-1}$ configurations with core polarization is now being carried out,[19] where r denotes the $p_{3/2}$, $p_{1/2}$, and $f_{5/2}$ orbits.

The broken-pair model[13] was used to calculate the $\rho^{tr}(r)$ for the $0^+_{g.s.}\rightarrow 2_1^+$ transition in ^{58}Ni. The $0\hbar\omega$ contribution is very small, whereas the $2\hbar\omega$ contribution plays a dominant role in reproducing the surface peak, in contrast to the present calculations in which the $0\hbar\omega$ contribution also plays the decisive role. The higher $\hbar\omega$ $(>2\hbar\omega)$ contributions are not considered in the broken-pair model.

It should be pointed out that the absolute value of $\rho^{tr}(r)$ is underestimated typically by a factor of 2 in ^{58}Ni, when the M3Y is used. On the other hand, when the ST is employed, the magnitude around the surface seems to be reproduced well, except in ^{58}Ni, although the position of the peak shifts toward the interior region. Random-phase approximation is expected to increase the transition matrix elements for collective states and thus the $\rho^{tr}(r)$ around the surface region.

C. $0^+\rightarrow 2^+_{2,3}$

Transition charge densities for the second and third excited 2^+ states of ^{58,60,62,64}Ni are calculated with the M3Y interaction and are shown in Figs. 5 and 6, respectively. The effective charge of $e_n=1.0e$ is used in the crudest model. The transition densities differ not only from those for the transitions to the 2_1^+ states but also from nucleus to nucleus. There are a number of transitions which show a similar inside-peak transition density, however. Comparison with experiment is made for ^{58}Ni, the only nucleus for which the experimental datum is available. For the $0^+_{g.s.}\rightarrow 2_2^+$ transition in ^{58}Ni, both the

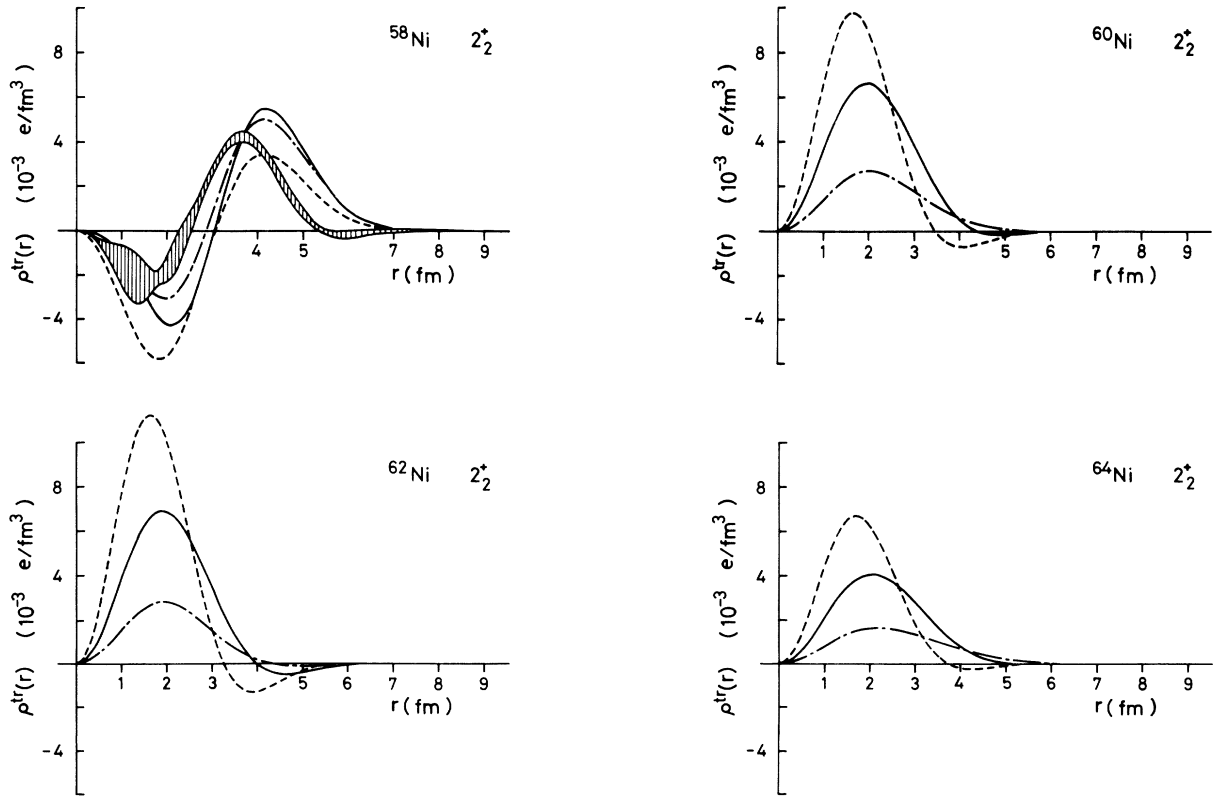

FIG. 5. Calculated and experimental (Ref. 4) transition charge densities $\rho^{tr}(r)$ for the second excited 2^+ states of even-mass Ni isotopes. The M3Y is used as the mixing interaction. See caption to Fig. 1.

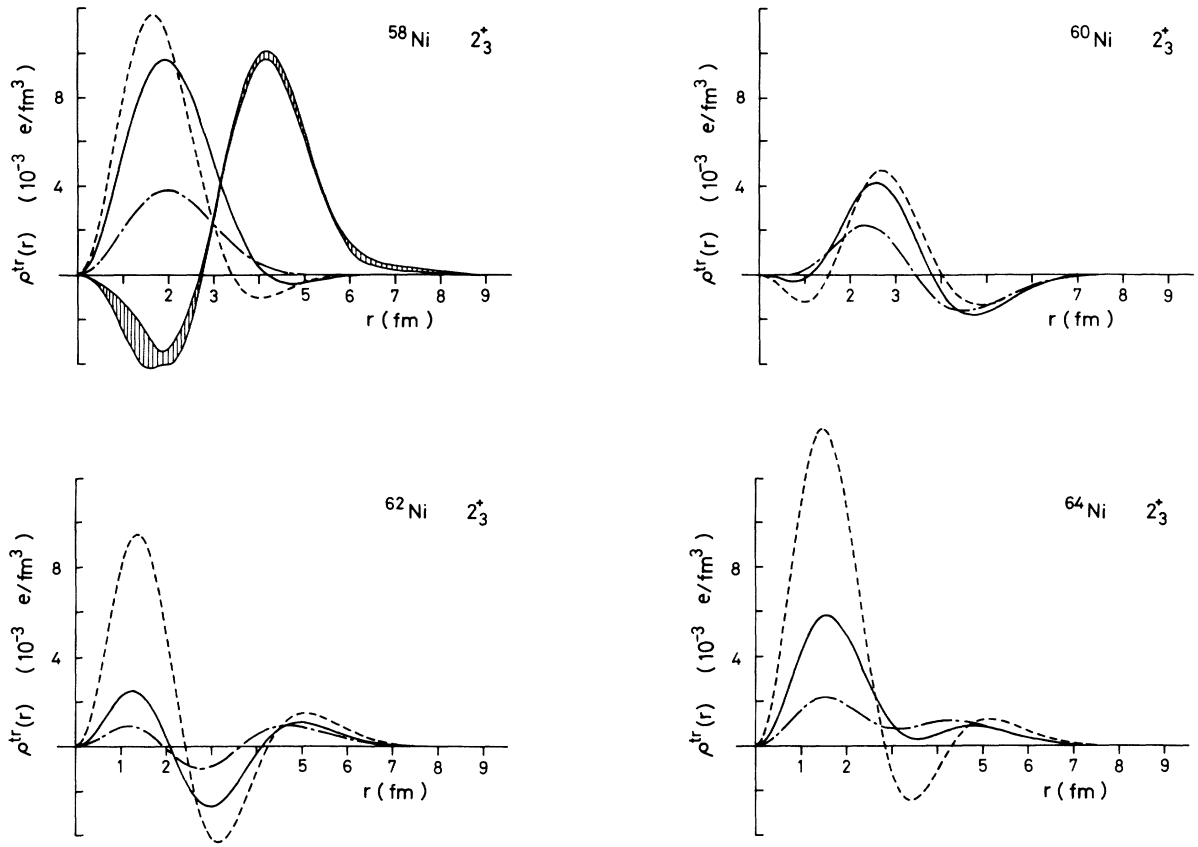

FIG. 6. Calculated and experimental (Ref. 4) transition charge densities $\rho^{tr}(r)$ for the third excited 2^+ states of even-mass Ni isotopes. The M3Y is used as the mixing interaction. See caption to Fig. 1.

$0\hbar\omega$ and $2\hbar\omega$ p-h excitations contribute almost equally and dominantly to the $\rho^{tr}(r)$, giving a peak both inside the nucleus and around the surface. The calculated $\rho^{tr}(r)$ for this transition is roughly consistent with experiment. For the $0^+_{g.s.} \rightarrow 2^+_2$ transitions in the other Ni isotopes, cancellation among each single-particle contribution occurs around the surface region. The $0\hbar\omega$ contribution becomes negligibly small and the higher $\hbar\omega$ excitations give significant contributions, generating an inside-peaked shape for the $\rho^{tr}(r)$. These $\rho^{tr}(r)$ are quite different from that of ^{58}Ni, suggesting that the structure of the 2^+_2 states in ^{60,62,64}Ni is changed by adding the neutrons in the model space. The experimental datum[4] for the $0^+_{g.s.} \rightarrow 2^+_3$ transition in ^{58}Ni shows a larger surface peak, whereas the calculations give a larger peak inside the nucleus rather than at the surface. Transition densities for the $0^+_{g.s.} \rightarrow 2^+_{1,2}$ transitions in Zn isotopes were analyzed[20] in terms of the vibrational model. A surface peak is predicted for the $0^+_{g.s.} \rightarrow 2^+_1$ transitions, but a large inside peak can be predicted for the forbidden $0^+_{g.s.} \rightarrow 2^+_2$ transitions, which is similar to the $\rho^{tr}(r)$ predicted for Ni isotopes in the present calculations. It would be interesting to make systematic comparison both with the vibrational-model calculations and with experimental data throughout Ni isotopes.

D. $0^+ \rightarrow 4^+_{1,2}$

Figures 7 and 8 present calculated transition charge densities for the first and second excited 4^+ states in ^{58,60,62,64}Ni, respectively. The constant effective charge of $e_n = 1.0e$ is assumed in the crudest model and then the $f_{5/2} \rightarrow p_{3/2}$ and the $f_{5/2} \rightarrow f_{5/2}$ transitions can participate in the $C4$ transitions. The former ($f \rightarrow p$) contributes predominantly to the $0^+_{g.s.} \rightarrow 4^+_1$ transitions. In the perturbation calculations, the $0\hbar\omega$ p-h excitations, which consist of the $f_{7/2} \rightarrow p$ transitions, give exactly the same r dependence in $\rho^{tr}(r)$ as the crudest model does. Furthermore, the $2\hbar\omega$ p-h excitations, which give the largest contribution to the $\rho^{tr}(r)$, turn out to be almost the same as the $0\hbar\omega$ ones, and higher $\hbar\omega$ excitations also give the similar r dependence. Therefore, it turns out that the p-h excitations are roughly incorporated into the constant effective charge. Similar results can be obtained with the other mixing interactions. For the $0^+_{g.s.} \rightarrow 4^+_1$ transition in ^{58}Ni, agreement between the calculation and experiment is remarkable, while for the $0^+_{g.s.} \rightarrow 4^+_2$ transition, as shown in Fig. 8, the calculation underestimates considerably.

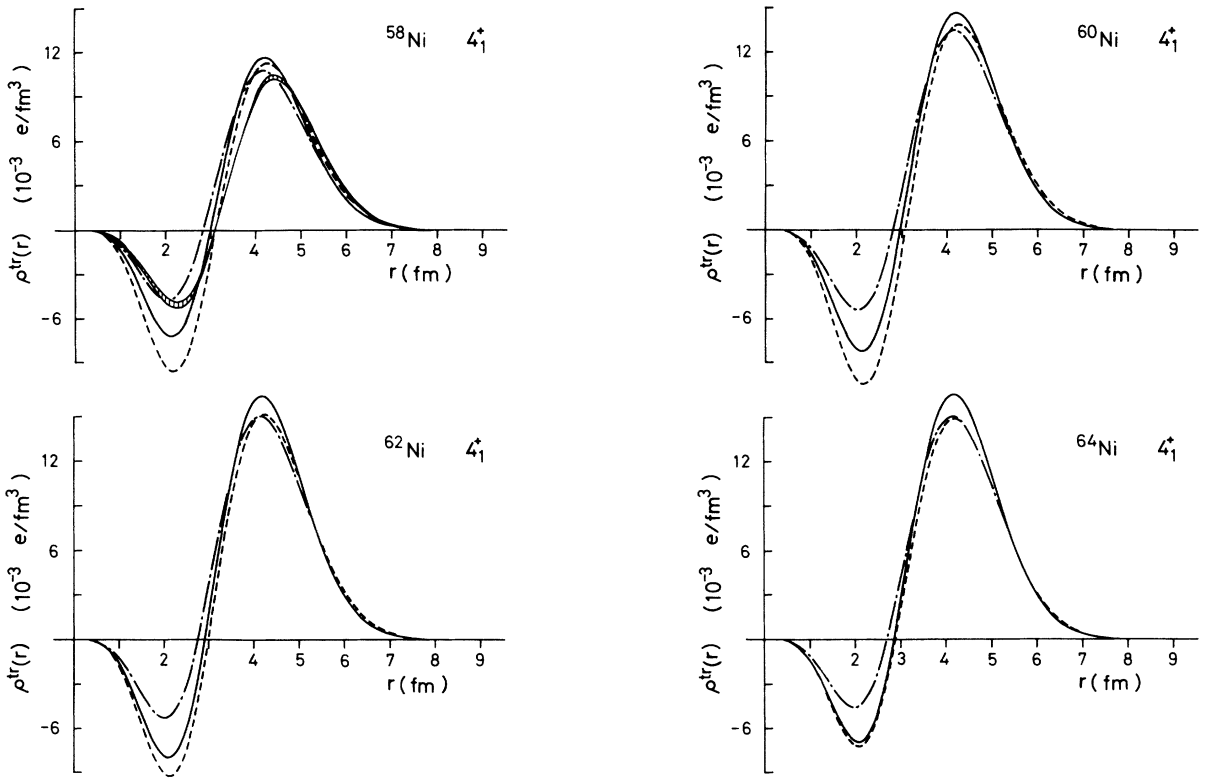

FIG. 7. Calculated and experimental (Ref. 4) transition charge densities $\rho^{tr}(r)$ for the first excited 4^+ states of even-mass Ni isotopes. The M3Y is used as the mixing interaction. See caption to Fig. 1.

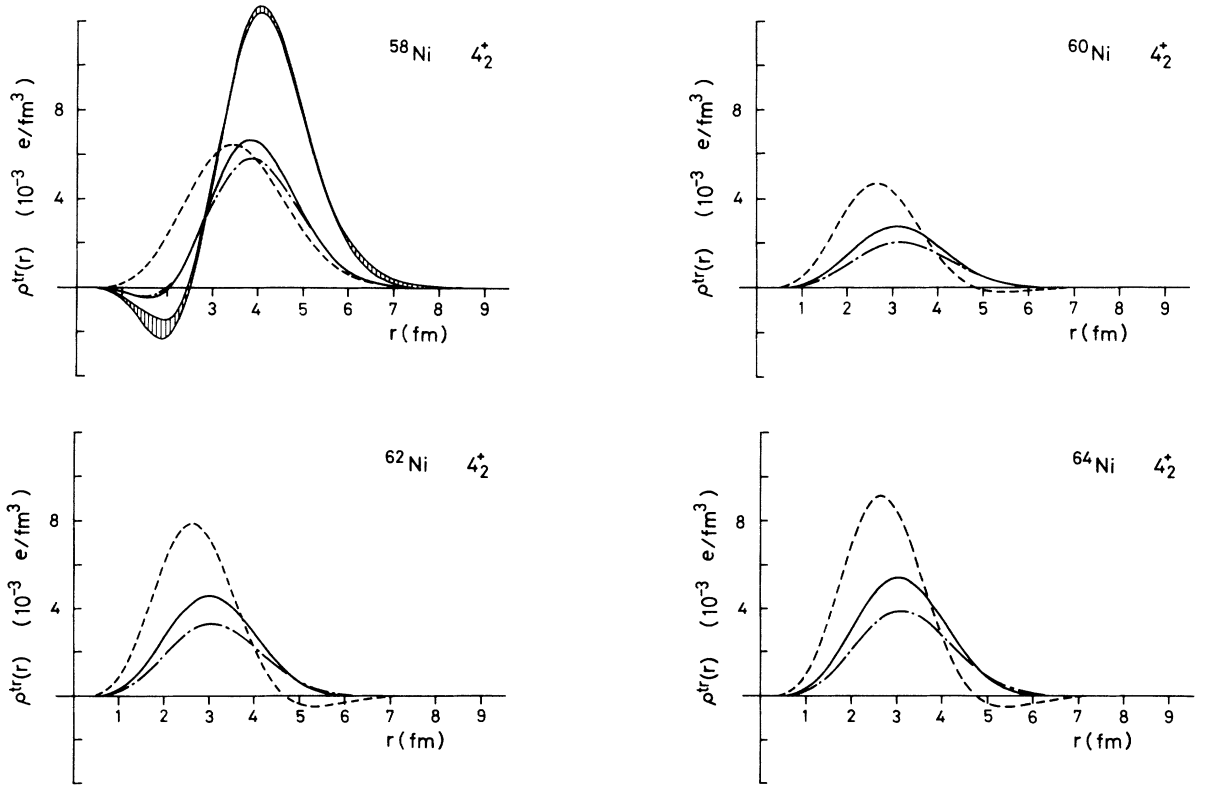

FIG. 8. Calculated and experimental (Ref. 4) transition charge densities $\rho^{tr}(r)$ for the second excited 4^+ states of even-mass Ni isotopes. The M3Y is used as the mixing interaction. See caption to Fig. 1.

III. SUMMARY AND CONCLUSIONS

Particle-hole excitations of the ^{56}Ni core are considered within the framework of the standard shell model of the $\nu(p_{3/2},p_{1/2},f_{5/2})^n$ configurations in order to interpret the transition charge densities of inelastic electron scattering for the excitation of $2^+_{1,2,3}$ and $4^+_{1,2}$ states in ^{58,60,62,64}Ni. Wave functions obtained by assuming the Adjusted Surface Delta Interaction (ASDI) of Koops and Glaudemans[9] are employed to calculate the one-particle density matrix element $\langle J_f\|u^{(\lambda)}(\alpha,\beta)\|J_i\rangle$. Effective one-particle transition matrix elements $(\alpha\|\bar{O}^{(\lambda)}\|\beta)$ are calculated by using a first-order perturbation theory which takes up to the $(\lambda+10)\hbar\omega$ excitation energy.

For the $0^+_{g.s.}\rightarrow 2^+_1$ transitions, both the $0\hbar\omega$ and $2\hbar\omega$ p-h excitation give important contributions to the $\rho^{tr}(r)$ overall region of r. Both contributions are added constructively around the surface region, while they cancel each other inside the nucleus, producing a relatively sharp peak around the surface. This gives rise to fairly nice agreement between calculation and experiment. The higher $\hbar\omega$ components enhance the magnitude of the surface peak, but they simultaneously have non-negligible contributions inside the nucleus, which tend to deteriorate appreciably agreement between calculation and experiment. There exists mixing-interaction dependence. The M3Y underestimates the magnitude of the peak, whereas the ST seems to give the correct magnitude except for ^{58}Ni. It is difficult to reproduce the $\rho^{tr}(r)$ inside the nucleus.

For the $0^+_{g.s.}\rightarrow 4^+_1$ transitions, the p-h excitations up to $4\hbar\omega$ are dominant in the matrix elements and contributions from each $k\hbar\omega$ excitation give similar r dependence in the $\rho^{tr}(r)$. There appears a larger peak at the surface and a smaller peak inside the nucleus with opposite sign. This feature can be changed neither by including the higher $\hbar\omega$ excitations nor by assuming the other mixing interactions. Agreement between the calculation and experiment in ^{58}Ni is remarkable.

For the transitions to the $2^+_{2,3}$ and 4^+_2 states, cancellation can occur in the summation over α and β in

$$\sum_{\alpha\beta}\langle J_f\|u^{(\lambda)}(\alpha,\beta)\|J_i\rangle(\alpha\|\bar{O}^{(\lambda)}\|\beta)\ ,$$

which depends on r. This suggests that the transition matrix element is sensitive to the slight change in the wave functions. Thus, the transitions to the $2^+_{2,3}$ and 4^+_2 states might be used in order to extract useful information on the nuclear-structure studies, if systematic comparison with experiment can be made.

In conclusion, it is shown that the perturbative approach works very well in describing the $\rho^{tr}(r)$ around the surface region for the 2^+_1 and 4^+_1 states, but it does not always give a reasonable description for the transitions to the $2^+_{2,3}$ and 4^+_2 states and neither for the $\rho^{tr}(r)$ in the interior region. The diversity of $\rho^{tr}(r)$ inside the nucleus may be related to short-range correlations which are not yet taken into account in the present approach. Systematic comparison with experiment is therefore invaluable for further discussion and experiment covering the wide mass region with sufficient q range is highly anticipated.

ACKNOWLEDGMENTS

One of the authors (A.Y.) is indebted to Professor H. Horie and Professor L. Zamick for informative discussions on effective charges. He also thanks Professor H. P. Blok for communicating to him the experimental data on ^{58}Ni and Professor K. Itoh and Professor T. Saito for providing him experimental data taken at Tohoku University with helpful comments. Thanks also go to Professor P. W. M. Glaudemans and Dr. A. G. M. van Hees for giving him their results concerning the shell-model calculations of Ni isotopes with the extended model space. The numerical calculations were carried out with the HITAC M-682H/M-680H system at the Computer Center of the University of Tokyo.

APPENDIX

The transition charge density $\rho_\lambda(r)$ can be expanded into a Fourier-Bessel series within the interval $r\le R_c$;

$$\rho_\lambda(r)=\begin{cases}\sum_{\mu=1}^{\mu_{max}} A_\mu\alpha_\mu(r), & \text{for } r\le R_c\\ 0, & \text{for } r>R_c\ ,\end{cases}\tag{A1}$$

where $\alpha_\mu(r)$ is defined by using the spherical Bessel function j_λ, as $\alpha_\mu(r)=\xi_\mu j_\lambda(\xi_\mu r)$, A_μ is its coefficient to be determined experimentally, and R_c is the cutoff radius chosen rather arbitrarily.[2] ξ_μ satisfies the following condition:

$$j_{\lambda-1}(\xi_\mu R_c)=0\ .\tag{A2}$$

The variance in $\rho(r)$, denoted by $\delta\rho(r)$, is calculated according to the rules of error propagation:

$$|\delta\rho(r)|^2=\left|\sum_{\mu=1}^{\mu_{max}}\frac{\partial\rho(r)}{\partial A_\mu}\delta A_\mu\right|^2=\left|\sum_{\mu=1}^{\mu_{max}}\alpha_\mu\delta A_\mu\right|^2\le\sum_{\mu=1}^{\mu_{max}}|\alpha_\mu|^2|\delta A_\mu|^2\ ,\tag{A3}$$

where δA_μ is the variance in A_μ, which originates from the uncertainties in the measured data and from the lack of knowledge on the data beyond higher momentum transfer region. Taking the square root of Eq. (A3), we have

$$\delta\rho(r)=\left[\sum_{\mu=1}^{\mu_{max}}|\alpha_\mu|^2|\delta A_\mu|^2\right]^{1/2}\ .\tag{A4}$$

Thus, the upper and lower limits of experimental data can be expressed as

$$\rho(r)_{upper}=\rho(r)+\delta\rho(r)\ ,\qquad \rho(r)_{lower}=\rho(r)-\delta\rho(r)\ ,\tag{A5}$$

respectively.

[1]T. deForest and J. Walecka, Adv. Phys. **15**, 1 (1966); H. Überall, *Electron Scattering From Complex Nuclei* (Academic, New York, 1971).
[2]J. Heisenberg, Adv. Nucl. Phys. **12**, 61 (1981); private communication.
[3]B. Frois *et al.*, Phys. Lett. **122B**, 347 (1983).
[4]H. Blok, Ph.D. dissertation, Vrije Universiteit Amsterdam, 1986; H. P. Blok, private communication.
[5]H. Horie and A. Arima, Phys. Rev. **99**, 778 (1955).
[6]H. Noya, A. Arima, and H. Horie, Prog. Theor. Phys. Suppl. **8**, 33 (1958)
[7]M. Horiike and H. Horie, Nucl. Phys. **A277**, 270 (1977).
[8]Y. Horikawa, T. Hoshino, and A. Arima, Nucl. Phys. **A278**, 297 (1977).
[9]J. E. Koops and P. W. M. Glaudemans, Z. Phys. A **280**, 181 (1977).
[10]H. Horie, J. Phys. Soc. Jpn. Suppl. **34**, 461 (1973).
[11]P. Federman and L. Zamick, Phys. Rev. **177**, 1534 (1969).
[12]A. Rimini, in *Theory of Nuclear Structure: Trieste Lectures 1969* (International Atomic Energy Agency, Vienna, 1970), p. 713.
[13]W. Hengeveld, K. Allaart, and W. H. Dickhoff, Nucl. Phys. **A435**, 381 (1985).
[14]A. Yokoyama and K. Ogawa, Phys. Rev. C **39**, 2458 (1989).
[15]W. G. Love. in *The (p,n) Reaction and the Nucleon-Nucleon Force*, edited by C. D. Goodman, S. M. Austin, S. D. Bloom, J. Rapaport, and G. R. Satchler (Plenum, New York, 1980), p. 23.
[16]J. P. Schiffer and W. W. True, Rev. Mod. Phys. **38**, 191 (1976).
[17]A. G. M. van Hees, P. W. M. Glaudemans, and B. C. Metsch, Z. Phys. A **293**, 327 (1979).
[18]R. B. G. Mooy and P. W. M. Glaudemans, Nucl. Phys. **A435**, 461 (1985).
[19]A. Yokoyama, J. G. L. Booten, and A. G. M. van Hees (unpublished).
[20]R. Neuhausen, Nucl. Phys. **A282**, 125 (1977).